Local entropies across the Mott transition in an exactly solvable model

Luke Yeo[*] and Philip W. Phillips[†]

Department of Physics, University of Illinois at Urbana-Champaign, Urbana, 61801 Illinois, USA

(Received 31 January 2019; published 22 May 2019)

We study entanglement in the Hatsugai-Kohmoto model, which exhibits a continuous interaction-driven Mott transition. By virtue of the all-to-all nature of its center-of-mass-conserving interactions, the model lacks dynamical spectral weight transfer, which is the key to the intractability of the Hubbard model for $d > 1$. In order to maintain a nontrivial Mott-like electron propagator, SU(2) symmetry is preserved in the Hamiltonian, leading to a ground state that is mixed on both sides of the phase transition. Because of this mixture, even the metal in this model is unentangled between any pair of sites, unlike free fermions whose ground state carries a filling-dependent site-site entanglement. We focus on the scaling behavior of the one- and two-site entropies s_1 and s_2, as well as the entropy density s, of the ground state near the Mott transition. At low temperatures in the two-dimensional Hubbard model, Walsh *et al.* [Phys. Rev. B **99**, 075122 (2019)] observed numerically that s_1 and s increase continuously into the metal, across a first-order Mott transition. In the Hatsugai-Kohmoto model, s_1 acquires the constant value ln 4 even at the Mott transition. On the other hand, s_2 and s each act as a sharp signal of the Mott transition, in any dimension, by decreasing at the transition into the metal. Specifically, we find that in one dimension, s_2 and s exhibit kinks at the transition while in two dimensions, only s exhibits a kink.

DOI: 10.1103/PhysRevD.99.094030

I. INTRODUCTION

It is well known for the Hubbard model that in the vicinity of half filling, adding and removing electrons changes [1–3] the spectrum at all energies. This state of affairs obtains because electrons are not the propagating degrees of freedom (d.o.f.). For example, it has been known since the early work of Harris and Lange [1] in 1967 that the low-energy spectral weight is not determined solely by the number of sites, a static quantity, but additionally depends on microscopic parameters in the Hamiltonian, specifically the ratio of the hopping, t, to the on-site interaction, U. This dependence, dubbed dynamical spectral weight transfer (DSWT) [2–4], renders the ground state adiabatically distinct from a Fermi liquid because in such systems no dynamical corrections to the spectral weight exist. That is, simply counting electrons exhausts the spectral weight. It is this dynamical mixing that makes the Hubbard model nontrivial and gives rise to a slew of nontrivial properties, in particular 1) an oxygen K-edge absorption [5,6] spectrum that increases faster than twice the doping level, 2) an integrated weight of the optical conductivity [7,8] in the lower Hubbard band that exceeds the nominal doping level, and 3) an upper cutoff on the integral of the optical conductivity, for recovery of the superfluid density, of $O(100\Delta)$, where Δ is the superconducting gap [9–11]. In metals described by Fermi liquid theory, integrating the optical conductivity to $O(\Delta)$ is sufficient to recover the superfluid density. All such deviations can be understood [2–4] within the context of the Hubbard model as a direct consequence of t/U corrections to the spectral weight or the optical conductivity.

As a result of DSWT, exact statements about the $d > 1$ Hubbard model are scarce. To alleviate this problem, we consider a simplification. Such a simplification would be ideal in the context of modern probes of strongly interacting matter such as the entanglement entropy. In this paper, we evaluate a measure of the entanglement in an exactly solvable model [12,13] exhibiting a second-order Mott transition. In so doing, we show that in addition to the entanglement entropy in free systems, which has been studied extensively [14–24], local entanglement in strongly correlated matter also exhibits key signatures [25,26] at phase transitions. Whereas the canonical model for such a transition—the Hubbard model—remains intractable in general, the Hatsugai-Kohmoto [12,13] (HK) model is exactly solvable. The model considers electrons interacting on a lattice with a limited class of all-to-all interactions. In one space dimension, a scaling analysis shows that both interaction- and density-driven transitions in the HK model lie in the same universality class as the density-driven transition in the Hubbard model [27,28]. Although markedly different from the Hubbard model, the HK model retains one crucial signature of the Mott transition: a retarded single-particle electron propagator whose real part

[*]lukeyeo2@illinois.edu
[†]dimer@illinois.edu

vanishes at zero energy. The existence of zeros is the hallmark of Mott insulation [3,29,30]. Propagators with zeros fail to satisfy the Luttinger sum rule for the ground state [31] and hence are not adiabatically connected to Fermi liquids.

In this paper, we analyze the Mott transition in the HK model from the perspective of local entropies. These are the two-point entanglement entropy between a pair of lattice sites, the entropy density s, and the single-site (two-site) entropy s_1 (s_2) of the ground state reduced to one (two) lattice site(s). Our work is motivated in part by a recent analysis of the latter quantities in the Hubbard model [25]. Two salient features of the HK model are its 1) mixed (i.e., degenerate) ground state and 2) infinite range interactions, to be contrasted with the Hubbard model's 1) pure ground state and 2) local interactions. For a pure state, entanglement entropy (across a bipartition in position space) measures delocalization of the wave function, which appears as itineracy in linear response [16,17]. Mixed states, on the other hand, carry both classical and quantum correlations, which are generally difficult to distinguish [32]. In low-dimensional Hilbert spaces, however, the entanglement of formation is analytically accessible; we utilize the low-dimensional nature of fermionic modes to compute the entanglement entropy between d.o.f. localized on a pair of lattice sites. In the larger Hilbert space setting, we study the local entropies s_1 and s_2 in relation to the entropy density s. Since the former quantities, s_1 and s_2, result from position-space bipartitions, they necessarily carry some of the entropy obtained by tracing over delocalized states in the ground-state ensemble. The latter quantity, s, cannot encode such quantum correlations in position space, so the discrepancy between them serves as a probe of entanglement near the Mott transition in the HK model.

II. MOTTNESS

The model [12,33] we analyze has long-range all-to-all nonlocal interactions with standard tight-binding hoppings,

$$H = -t\sum_{\langle j,l\rangle,\sigma}(c^\dagger_{j\sigma}c_{l\sigma} + \text{H.c.}) - \mu\sum_{j\sigma}c^\dagger_{j\sigma}c_{j\sigma} + \frac{U}{N}\sum_{j_1..j_4}\delta_{j_1+j_3,j_2+j_4}c^\dagger_{j_1\uparrow}c_{j_2\uparrow}c^\dagger_{j_3\downarrow}c_{j_4\downarrow}, \quad (1)$$

where the first and second terms denote the local hopping, t and chemical potential, μ. The last term is the infinite-range Hubbard-like interaction U; this term is nonzero for electrons that scatter in such a way that their position vectors satisfy the constraint of center-of-mass conservation given by $j_1 + j_3 = j_2 + j_4$. This model predates the SYK [34,35] model by 2 years, though it is considerably less studied. Although both models contain all-to-all nonlocal interactions, the current model is exactly solvable as a result of the conservation of the center of mass in the interaction term. The integrability of this model, without resorting to a $1/N$ expansion as in the SYK model [34,35], is best seen in momentum space

FIG. 1. Phase diagram of the HK model at zero temperature and half filling, as the interaction strength U is tuned from the noninteracting point $U = 0$ across the metal-insulator transition at $U = W$.

$$H = \sum_{\vec{k}}H_{\vec{k}} = \sum_{\vec{k}}(\xi(\vec{k})(\hat{n}_{\vec{k}\uparrow} + \hat{n}_{\vec{k}\downarrow}) + U\hat{n}_{\vec{k}\uparrow}\hat{n}_{\vec{k}\downarrow}), \quad (2)$$

from which it is clear that the kinetic and potential energy terms commute. In momentum space, the momenta are summed over a square Brillouin zone $[-\pi,\pi)^d$, within which the quasiparticle spectrum $\xi_k = \epsilon_k - \mu$ is set by the dispersion $\epsilon_k = -(W/2d)\sum_{\mu=1}^{d}\cos k^\mu$ with bandwidth W and offset by a chemical potential μ. Here $n_{k\sigma} = c^\dagger_{k\sigma}c_{k\sigma}$ is the fermion number operator for the mode with momentum k and spin $\sigma = \uparrow,\downarrow$. We consider the system at half filling, fixed by $\mu = U/2$. As depicted in Fig. 1, the ground state is metallic for $0 < U < W$, insulating for $U > W$, and undergoes an interaction-driven metal-insulator transition at $U = W$. The phase transition is sharp only at zero temperature, so we work at $T = 0$ throughout.

The retarded single-particle fermion propagator is related by analytic continuation to the zero-temperature Euclidean propagator. For a fermion in quantum state (k,σ) in the HK model,

$$G_{k\sigma}(i\omega) \equiv -\int d\tau\langle c_{k\sigma}(\tau)c^\dagger_{k\sigma}(0)\rangle e^{i\omega\tau} \quad (3)$$

$$= \frac{1-\langle n_{k\bar{\sigma}}\rangle}{i\omega - \xi_k} + \frac{\langle n_{k\bar{\sigma}}\rangle}{i\omega - (\xi_k + U)} \quad (4)$$

whose pole in the upper (lower) Hubbard band carries a spectral weight equal to the probability $p = \langle n_{k\bar{\sigma}}\rangle$ $(1-p)$ that a fermion occupies (does not occupy) the mode with identical momentum k and opposite spin $\bar{\sigma}$. It is customary to reformulate the Hubbard model [3] in terms of holons $\zeta_{k\sigma} = c_{k\sigma}(1 - n_{k\bar{\sigma}})$ and doublons $\eta = c_{k\sigma}n_{k\bar{\sigma}}$ which comprise the fermion $c_{k\sigma} = \zeta_{k\sigma} + \eta_{k\sigma}$. What distinguishes the HK from the Hubbard model is that the single-particle propagator

$$-\int d\tau\langle\zeta_{k\sigma}(\tau)\zeta^\dagger_{k\sigma}(0)\rangle e^{i\omega\tau} = \frac{1-\langle n_{k\bar{\sigma}}\rangle}{i\omega - \xi_k}, \quad (5)$$

$$-\int d\tau\langle\eta_{k\sigma}(\tau)\eta^\dagger_{k\sigma}(0)\rangle e^{i\omega\tau} = \frac{\langle n_{k\bar{\sigma}}\rangle}{i\omega - (\xi_k + U)}, \quad (6)$$

is strictly diagonal in terms of these operators because the cross term,

$$\langle \zeta_{k\sigma}(\tau)\eta^{\dagger}_{k\sigma}\rangle = 0 = \langle \eta_{k\sigma}(\tau)\zeta^{\dagger}_{k\sigma}\rangle, \tag{7}$$

identically vanishes. Consequently, the HK model, although it possesses an interaction-driven Mott transition, does not contain DSWT. As noted previously, it is this feature that makes the model tractable regardless of the spatial dimension. Whether there are other models that retain this feature but still remain tractable regardless of the spatial dimension is not known at present.

III. ENTANGLEMENT

Consider the ground state produced by the zero-temperature limit $\beta \equiv 1/T \to \infty$ of the equilibrium Gibbs state

$$e^{-\beta H}/Z = \otimes\, e^{-\beta H_k}/Z_k, \tag{8}$$

where $e^{-\beta H_k}/Z_k$ is the reduced density matrix for the mode k. Here $Z_k = \mathrm{tr} e^{-\beta H_k}$ and

$$e^{-\beta H_k} = \begin{pmatrix} 1 & & & \\ & e^{-\beta\xi_k} & & \\ & & e^{-\beta\xi_k} & \\ & & & e^{-\beta(2\xi_k+U)} \end{pmatrix} \tag{9}$$

is diagonal in the tensor product basis $\{|0,0\rangle, |0,1\rangle, |1,0\rangle, |1,1\rangle\}$ of the Hilbert space $\mathcal{H}_{k\uparrow} \otimes \mathcal{H}_{k\downarrow}$.

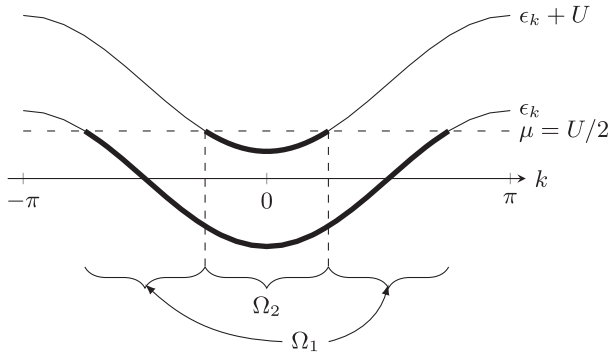

FIG. 2. Upper and lower Hubbard bands of the one-dimensional HK model in the metallic phase $U < W$. Shaded segments indicate occupied momenta. Ω_2 labels the doubly occupied region and Ω_1 the singly occupied region.

Then $e^{-\beta H_k}/Z_k$ is separable across $\mathcal{H}_{k\uparrow}$ and $\mathcal{H}_{k\downarrow}$, and likewise $e^{-\beta H}/Z$ is separable across $\mathcal{H}_{\uparrow} = \otimes_k \mathcal{H}_{k\uparrow}$ and $\mathcal{H}_{\downarrow} = \otimes_k \mathcal{H}_{k\downarrow}$, showing that no entanglement is present between the spin-up and -down sectors of $e^{-\beta H}/Z$. Notice however that $e^{-\beta H_k}/Z_k$ cannot be written as $\rho^{k\uparrow} \otimes \rho^{k\downarrow}$, and thereby implements classical correlations between the spin sectors. We will see that reduced states on one or two sites, instead, have completely uncorrelated spin sectors. Since $\langle n_{k\sigma}\rangle$ is a good quantum number, the ground state at zero temperature can be deduced from

$$\rho^k \equiv \lim_{\beta\to\infty} e^{-\beta H_k}/Z_k = \begin{cases} |0\rangle\langle 0|_{\uparrow} \otimes |0\rangle\langle 0|_{\downarrow} & \text{if } \xi_k > 0, \\ \frac{1}{2}|1\rangle\langle 1|_{\uparrow} \otimes |0\rangle\langle 0|_{\downarrow} + \frac{1}{2}|0\rangle\langle 0|_{\uparrow} \otimes |1\rangle\langle 1|_{\downarrow} & \text{if } \xi_k < 0 \quad \text{and} \quad \xi_k + U > 0, \\ |1\rangle\langle 1|_{\uparrow} \otimes |1\rangle\langle 1|_{\downarrow} & \text{if } \xi_k < 0 \quad \text{and} \quad \xi_k + U < 0, \end{cases} \tag{10}$$

such that modes k with $\xi_k > 0$ are unoccupied, those with $\xi_k < 0$ and $\xi_k + U > 0$ are singly occupied, and those with $\xi_k < 0$ and $\xi_k + U < 0$ are doubly occupied. In the metallic phase with $U < W$, the ground state forms an inner doubly occupied Fermi volume Ω_2 in which $\langle n_{k\sigma}\rangle = 1$ and an outer singly occupied shell Ω_1 in which $\langle n_{k\sigma}\rangle = 1/2$, as depicted in Fig. 2. The ground state is indeed half filled since $2|\Omega_2| + |\Omega_1| = (2\pi)^d$ is preserved. In terms of the number of modes N_i in Ω_i, this half-filling condition reads $2N_2 + N_1 = L^d$, and in terms of the fraction of modes singly or doubly occupied $n_i = N_i/L^d$ it reads $2n_2 + n_1 = 1$. As the phase boundary $U = W$ is approached from the metallic side, Ω_2 vanishes and Ω_1 covers the entire Brillouin zone. This state persists throughout the insulating phase with $U > W$. On the other side of the phase diagram, Ω_1 vanishes in the noninteracting limit $U \to 0$. In each phase, the singly occupied modes $k \in \Omega_1$ form a mixed sector of the ground state. The reduced state ρ^k on each singly occupied mode has nonvanishing mutual information $I(k\uparrow : k\downarrow) = \ln 2$ between spin sectors. As a result, ρ^k indeed carries classical correlations while being unentangled. Distributing the momentum (tensor) product over the mixing sum in $\rho^{k\in\Omega_1}$, we see that the ground state takes the form of a uniform mixture over paramagnetic spin configurations

$$\rho = p_\pi \sum_{\sum_q \pi(q)=0} |\pi\rangle\langle\pi| \tag{11}$$

$$|\pi\rangle = \prod_{q\in\Omega_1} c^{\dagger}_{q\pi(q)} \prod_{k\in\Omega_2} (c^{\dagger}_{k\uparrow} c^{\dagger}_{k\downarrow})|0\rangle, \tag{12}$$

where each of the $\binom{N_1}{N_1/2} = 1/p_\pi$ permutations $\pi : \Omega_1 \to \{\uparrow, \downarrow\}$ maps the N_1 modes in Ω_1 to a paramagnetic spin

configuration, resulting in the Bloch state $|\pi\rangle$. The ground state in the insulating phase has Ω_1 covering the entire Brillouin zone, such that $N_1 = L^d$ and the number of modes N_2 in the doubly occupied region Ω_2 is zero.

Within the singly occupied region Ω_1, the real part of the retarded propagator at zero temperature takes the form

$$\mathrm{Re}G^{\mathrm{R}}_{k\sigma}(\omega) = \frac{1}{2}\mathcal{P}\left[\frac{1}{\omega - \epsilon_k + U/2} + \frac{1}{\omega - \epsilon_k - U/2}\right], \quad (13)$$

given by continuing $i\omega \mapsto \omega + i0^+$. At zero energy, the real part $\mathrm{Re}G^{\mathrm{R}}_{k\sigma}(\omega = 0)$ vanishes on the surface $\{k \in [-\pi, \pi)^d : \epsilon_k = 0\}$ which always lies inside the region Ω_1. It is this zero surface [3,29,30] that is the hallmark of Mottness. Because the region Ω_1 is finite for all couplings $U > 0$, the quasiparticle description is valid only at the noninteracting point $U = 0$ and breaks down everywhere else in the phase diagram.

From the point of view of position space, each delocalized Bloch wave function in the ground-state ensemble appears entangled. Formally the Fourier transform $\otimes_k \mathcal{H}_{k\sigma} \to \otimes_j \mathcal{H}_{j\sigma}$ acts as a global entangling map within each spin sector [16,17]. Since the ground state ρ is spin separable, it remains similarly separable after a Fourier transform to position space, and entanglement in ρ can be present only within each spin sector. Entanglement between the spin-σ modes localized on sites j and j' can be determined conclusively from the reduced state $\rho^{jj'\sigma}$ on $\mathcal{H}_{j\sigma} \otimes \mathcal{H}_{j'\sigma}$. We refer to entanglement between these modes as two-point entanglement. Following Zanardi's notation in Ref. [16], conservation of particle number mandates that the reduced state be

$$\rho^{jj'\sigma} = \begin{pmatrix} u & & & \\ & w_1 & z & \\ & z^* & w_2 & \\ & & & v \end{pmatrix} \quad (14)$$

in the tensor product basis $\{|0,0\rangle, |0,1\rangle, |1,0\rangle, |1,1\rangle\}$ of $\mathcal{H}_{j\sigma} \otimes \mathcal{H}_{j'\sigma}$, where the matrix elements are given by

$$z = \langle c^\dagger_{j\sigma} c_{j'\sigma}\rangle, \quad (15)$$

$$w_1 = \langle (1 - n_{j\sigma}) n_{j'\sigma}\rangle, \quad (16)$$

$$w_2 = \langle n_{j\sigma}(1 - n_{j'\sigma})\rangle, \quad (17)$$

$$v = \langle n_{j\sigma} n_{j'\sigma}\rangle, \quad (18)$$

$$u = 1 - w_1 - w_2 - v. \quad (19)$$

At half filling where $\langle n_{j\sigma}\rangle = 1/2$, translation invariance obtains

$$w_1 = w_2 = 1/2 - v \quad (20)$$

with $u = v$, and Wick contraction within the ground-state ensemble (of pure Bloch wave functions) obtains

$$v = (1/2)^2 - |z|^2. \quad (21)$$

That $|z|$ must be sufficiently large, in order that $\rho^{jj'\sigma}$ be entangled, can be seen from the Peres-Horodecki criterion [14]: the two-qubit state ρ^{AB} is separable if and only if its partial transpose $(\rho^{AB})^{\mathsf{PT}}$ has no negative eigenvalues. Since $\rho^{jj'\sigma}$ is written in the tensor product basis, transposition in the second (inner) Hilbert space $\mathcal{H}_{j'\sigma}$ can be read off as

$$\rho^{jj'\sigma} \mapsto (\rho^{jj'\sigma})^{\mathsf{PT}} = \begin{pmatrix} u & & & z \\ & w_1 & & \\ & & w_2 & \\ z^* & & & v \end{pmatrix}. \quad (22)$$

The probability spectrum is mapped to $\{w_1, w_2, (1/2)^2 - |z|^2 \pm |z|\}$, thereby developing a negative eigenvalue if

$$|z| > z_0 \equiv (\sqrt{2} - 1)/2 \approx 0.207. \quad (23)$$

Turning to momentum space to compute $|z|$, we find that

$$z = \frac{1}{L^d}\sum_{kk'} \langle c^\dagger_{k\sigma} c_{k'\sigma}\rangle e^{-i(k\cdot j - k'\cdot j')} \quad (24)$$

$$= \frac{1}{L^d}\sum_{k} \langle n_{k\sigma}\rangle e^{-ik\cdot(j-j')} \quad (25)$$

$$= \frac{1}{2}\frac{1}{L^d}\sum_{k\in\Omega_1} e^{-ik\cdot(j-j')} + \frac{1}{L^d}\sum_{k\in\Omega_2} e^{-ik\cdot(j-j')}. \quad (26)$$

Writing the momentum vector with constant components $\vec{\pi}_\mu = \pi$, the sum on Ω_1 reduces to the sum $\mathcal{J}(j - j') \equiv \frac{1}{L^d}\sum_{k\in\Omega_2} e^{-ik\cdot(j-j')}$ on Ω_2 as

$$\frac{1}{L^d}\sum_{k\in\Omega_1} e^{-ik\cdot(j-j')} = \frac{1}{L^d}\left(\sum_{k\in \mathrm{BZ}} - \sum_{k\in\Omega_2} - \sum_{(k-\vec{\pi})\in\Omega_2}\right) e^{-ik\cdot(j-j')} \quad (27)$$

$$= 0 - \mathcal{J}(j-j') - e^{-i\vec{\pi}\cdot(j-j')}\mathcal{J}(j-j') \quad (28)$$

where $e^{-i\vec{\pi}\cdot(j-j')}$ is -1 if $\|j - j'\|_1$ is odd, but is $+1$ if $\|j - j'\|_1$ is even. Then

$$z = \begin{cases} 0 & \text{if } \|j - j'\|_1 \text{ is even,} \\ \mathcal{J}(j - j') & \text{if } \|j - j'\|_1 \text{ is odd.} \end{cases} \tag{29}$$

In order to evaluate the domain-restricted sum analytically, we work in the thermodynamic limit near the Mott transition, where the Fermi volumes have spherical symmetry and the sums approach integrals. As shown in Fig. 2, the boundary of Ω_2 is the locus of $\epsilon_k + U = \epsilon_{\vec{\pi}+k}$. In the metallic phase near the Mott transition, where $U = W(1 - \delta u)$ for small $\delta u > 0$, Ω_2 is a d-dimensional ball $B^d(k_{F,2}, \vec{0})$ centered on the origin with radius $k_{F,2} = \sqrt{2d(1 - U/W)} \equiv \sqrt{2d\delta u}$. In this regime, the fraction of modes that are doubly occupied $n_2 = N_2/L^d \ll 1$ is a natural small parameter. The domain-restricted integral reduces to

$$\mathcal{J}(j - j') \to \int_{k \in \Omega_2} \frac{d^d k}{(2\pi)^d} e^{-ik\cdot(j-j')} \tag{30}$$

$$= \left(\frac{k_{F,2}/2\pi}{|j - j'|}\right)^{d/2} J_{d/2}(k_{F,2}|j - j'|) \tag{31}$$

$$\sim n_2 \tag{32}$$

at leading order in $n_2 \ll 1$. Then near the Mott transition, $n_2 \not> z_0$ so $\rho^{jj'\sigma}$ is separable there. $z = \mathcal{J}(j - j')$ crosses the threshold value z_0 only in one dimension $d = 1$, where Eq. (31) holds also away from the Mott transition, for neighboring sites $j - j' = 1$ and deep in the metallic phase at $U/W \approx 0.7835$. Free lattice fermion ground states similarly have $z < z_0$ in any dimension $d > 1$, so two-point entanglement cannot distinguish the state ρ in $d > 1$. In $d = 1$, however, the free ground state has $\mathcal{J}(j - j' = 1) > z_0$ as long as the lattice is extensively filled [16]. We conclude for $d = 1$ that the ground state ρ, in the vicinity of the Mott transition, is less entangled than any state with a free Fermi surface. For $d > 1$, the ground state ρ remains devoid of two-point entanglement—indistinguishable from free fermions.

Consider now the local entropies. As seen above, even the ground state in this model is a mixed state with both classical and quantum uncertainty. Whereas its quantum uncertainty—in the form of entanglement across bipartitions in position space—indicates itineracy, its classical uncertainty simply originates from an unbroken SU(2) symmetry. Now the presence of both classical and quantum uncertainty in the ground state ρ makes it difficult to isolate either portion [32], leaving us with hints of itineracy that are muddled by classical uncertainty. In this context, we consider two local entropies that signal the Mott transition—the entropy density s and the two-site entropy s_2—as well as one that does not signal the transition—the single-site entropy s_1. The local entropies,

$$s_1 \equiv S(\rho^j) = -\mathrm{tr}(\rho^j \ln \rho^j), \tag{33}$$

$$s_2 \equiv S(\rho^{\langle jj'\rangle}) = -\mathrm{tr}(\rho^{\langle jj'\rangle} \ln \rho^{\langle jj'\rangle}), \tag{34}$$

are von Neumann entropies of the reduced states $\rho^j = \mathrm{tr}_{i\neq j}\rho$ and $\rho^{\langle jj'\rangle} = \mathrm{tr}_{i\neq j,j'}\rho$ associated with the bipartitions $\mathcal{H}_j \otimes \mathcal{H}_{\bar{j}}$ and $(\mathcal{H}_j \otimes \mathcal{H}_{j'}) \otimes \mathcal{H}_{\overline{j,j'}}$ across position space, where j and j' are neighbors and the overline denotes the set complement on the lattice, whereas

$$s \equiv \frac{1}{L^d} S(\rho) = -\frac{1}{L^d} \mathrm{tr}(\rho \ln \rho) \tag{35}$$

is the entropy density of the full many-body ground state ρ and does not involve any bipartition of d.o.f. s_1 and s_2 are not entanglement entropies because the ground state ρ is not pure.[1] s_2 and $2s$ measure entropy on the same volume of phase space, each one bounded between zero and $\ln(\dim \mathcal{H}_j)^2 = \ln 16$, so the two quantities are readily comparable. However only s_2 is sensitive to the details of correlations in the ground state, for instance whether they are concentrated in position or momentum space. The subadditivity of the entropy requires that $2s_1 \geq s_2 \geq 2s$. The former bound is saturated only if $\rho^{\langle jj'\rangle} = \rho^j \otimes \rho^{j'}$ is uncorrelated between single-site subsystems, and the latter bound is saturated only if $\rho = \bigotimes_n \rho^{2n,2n+1}$ is uncorrelated between all (disjoint) two-site subsystems, with the latter implying the former due to translation invariance. Then any discrepancy between $2s$, $2s_1$, and s_2 indicates the presence of local correlations in the ground state, which may be entirely classical. The entropy density is obtained straightforwardly from the decomposition $\rho = \bigotimes_k \rho^k$, with ρ^k from Eq. (10), as

$$s = \frac{1}{L^d} \sum_k S(\rho^k) \tag{36}$$

$$= \frac{1}{L^d} \sum_{k \in \Omega_1} S(\rho^k) \tag{37}$$

$$= n_1 \ln 2 \tag{38}$$

$$= \ln 2 - (\ln 4) n_2 \tag{39}$$

where we used the additivity of entropy in the first line, the vanishing entropy of all pure states $\rho^{k\notin\Omega_1}$ in the second, the

[1] We are unable to perform a conclusive analysis of the entanglement structure of ρ, as was done for $\rho^{jj'\sigma}$, because the involved Hilbert space dimensions ($4 \otimes 4^{L^d-1}$ and $4^2 \otimes 4^{L^d-2}$) are larger than $2 \otimes 2$ and $2 \otimes 3$.

definition $n_1 = |\Omega_1/(2\pi)^d = N_1/L^d$ in the third, and the half-filling condition $n_1 + 2n_2 = 1$ in the final line.

The computation of s_1 and s_2 follows simply from the factorization of the associated reduced states $\rho^j = \rho^{j\uparrow} \otimes \rho^{j\downarrow}$ and $\rho^{\langle jj'\rangle} = \rho^{jj'\uparrow} \otimes \rho^{jj'\downarrow}$, which can be seen from the factorization of their matrix elements. That is, for operators O_σ localized on the spin-σ sector $\otimes_{j\in A}\mathcal{H}_{j\sigma}$ of $\mathcal{H}_A$, the matrix elements[2] of the reduced state ρ^A on subregion A factorize as

$$\langle O_\uparrow O_\downarrow\rangle_{\rho^A} = \langle O_\uparrow\rangle_{\rho^A}\langle O_\downarrow\rangle_{\rho^A}. \tag{41}$$

This factorization is shown in the Appendix. The conservation of particle number leaves $\rho^{j\sigma} = \mathrm{diag}(\langle 1 - n_{j\sigma}\rangle, \langle n_{j\sigma}\rangle) = \mathbb{1}_2/2$, with the latter equality set by half filling, such that $\rho^j = \mathbb{1}_4/4$ is maximally mixed with entropy

$$s_1 = \ln 4. \tag{42}$$

This is consistent with a direct computation of the double-occupancy density $\langle n_{j\uparrow}n_{j'\downarrow}\rangle = 1/4$,[3] which holds everywhere in the phase diagram and therefore does not signal the Mott transition. In the Hubbard model, it is precisely this quantity which changes discontinuously across the Mott transition [25]. The matrix elements of $\rho^{jj'\sigma}$ were found around Eq. (14), giving its entropy $S(\rho^{jj'\sigma}) \sim \ln 4 - 4(n_2)^2$ near the Mott transition, such that

$$s_2 \sim \ln 16 - 8(n_2)^2. \tag{43}$$

Relating $n_2 = |\Omega_2|/(2\pi)^d$ to the volume $|\Omega_2|$ of the d-ball with radius $k_{F,2}$ yields the scaling $n_2 \sim c_d(\delta u)^{d/2}$ near the Mott transition, where $c_d = (d/2\pi)^{d/2}/\Gamma(d/2+1)$. Then

$$s_2 \sim \ln 16 - 8(c_d)^2\delta u^d, \tag{44}$$

[2]Recall that the matrix elements of a reduced state ρ^A on $\mathcal{H}_A$ can be constructed, given a basis $|a\rangle \otimes |b\rangle$ of $\mathcal{H}_A \otimes \mathcal{H}_B$, from the expectation values

$$\langle |a\rangle\langle a'| \otimes \mathbb{1}_B\rangle_\rho = \langle |a\rangle\langle a'|\rangle_{\rho^A} = \langle a'|\rho^A|a\rangle \tag{40}$$

of operators $|a\rangle\langle a'| \otimes \mathbb{1}_B$ localized on $\mathcal{H}_A$.

[3]Hatsugai and Kohmoto [12] erroneously found a finite-size correction to $\langle n_{j\uparrow}n_{j'\downarrow}\rangle$ from inconsistent asymptotics. Their calculation amounts to counting $N_1(N_1-1)$ terms in the sum over $\{k, q \in \Omega_1 :\ k \neq q\}$ in the Fourier transform, but evaluating $\langle n_{k\uparrow}n_{q\downarrow}\rangle$ as $(1/2)^2$ in the sum. The latter quantity is instead $(1/2)^2/(1-1/N_1) = \binom{N_1-1}{(N_1-2)/2}/\binom{N_1}{N_1/2}$, found by counting the number of states $|\pi\rangle$ in the ensemble with $\langle n_{k\uparrow}\rangle_\pi = 1 = \langle n_{q\downarrow}\rangle_\pi$ for fixed $k, q \in \Omega_1$.

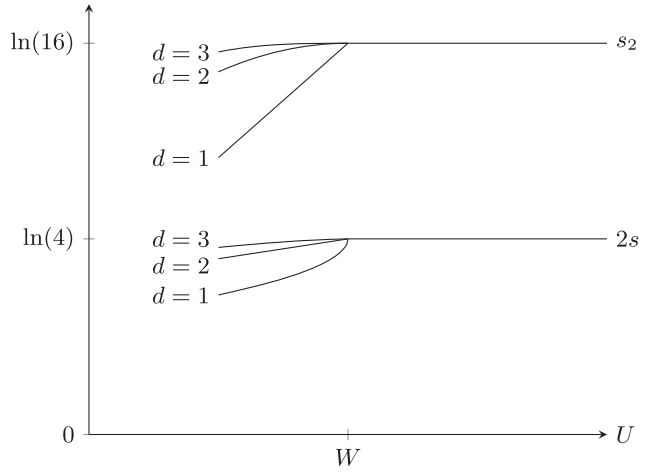

FIG. 3. Illustrative ground-state local entropies in the HK model at half filling, as the interaction strength U is tuned across the Mott transition at $U = W$. s is the entropy density of the full ground state ρ, and s_2 is the entropy of ρ reduced to two neighboring sites. The curves are exact only for $U \geq W$, with those in $U < W$ given by $U \nearrow W$ asymptotics.

$$2s \sim \ln 4 - (\ln 16)c_d\delta u^{d/2} \tag{45}$$

near the Mott transition, whereas $s_1 = \ln 4$ everywhere in the phase diagram.

As illustrated in Fig. 3, each local entropy deviates from its insulating value only at $U = W$, thereby signaling the Mott transition in the approach from the insulating phase. Both local entropies have a kink at the Mott transition in $d = 1$, only s has a kink there in $d = 2$ dimensions, and both quantities are otherwise smooth there. The decrease in the entropy density s is entirely explained by a reduced degeneracy of the ground state in the metallic phase. As discussed earlier, the entropy captured by s is generically mixed into s_2, with $s_2 \geq 2s$ by subadditivity. Then the decrease in the two-site entropy s_2 should, at least in part, be explained likewise. However, s_2 is substantially larger than $2s$ for $U \approx W$ and $U > W$, and their scaling exponents near the Mott transition are different. The spatial bipartition distinguishing the two local entropies is therefore significant; the decrease in the two-site entropy s_2 can be explained independently of the ground-state degeneracy. Given that the single-site entropy $s_1 = \ln 4$ is constant, the behavior of the two-site mutual information

$$I(j:j') \equiv S(\rho^j) + S(\rho^{j'}) - S(\rho^{\langle jj'\rangle}) = 2s_1 - s_2 \tag{46}$$

completely determines the behavior of the two-site entropy s_2, and $I(j:j')$ is itself bounded from below by all connected two-point correlation functions $\langle O_j O_{j'}\rangle - \langle O_j\rangle\langle O_{j'}\rangle$

between sites j and j'.[4] In the insulating phase, $s_2 = 2s_1$ so the mutual information vanishes and accordingly all connected j–j' correlation functions vanish. From Eq. (3) we know that two-point correlations turn on at the Mott transition from gapped insulator to gapless metal, so the mutual information $I(j:j') \gtrsim \langle c^\dagger_{j\sigma} c_{j'\sigma}\rangle \sim n_2$ must also turn on there. Consequently the two-site entropy s_2 must decrease from its value in the insulating phase, in a manner governed by two-point correlations. In the context of correlations and the single-site substructure of s_2, the local entropies s_2 and s are therefore independent.

IV. DISCUSSION

Dynamical spectral weight transfer, originating from dynamical double occupancy, is a fingerprint of the nontrivial propagating d.o.f. in the Hubbard model. We have studied the HK model of a Mott transition with static double occupancy, focusing our analysis on two-point entanglement and local entropies in its ground state near the phase transition. Static double occupancy directly results in a double-occupancy density $\langle n_{j\uparrow} n_{j\downarrow}\rangle$ that is constant across the phase diagram, thereby fixing the single-site entropy s_1 at the constant value $\ln 4$ even at the Mott transition. On the other hand, the two-site entropy s_2 and entropy density s serve as sharp signals of the Mott transition in any dimension d. They are constant in the insulating phase and decrease only when the interaction U is lowered past the transition at $U = W$. In one dimension, s_2 and s feature kinks at the Mott transition, reminiscent of the single-site entropy s_1 at pure-state quantum phase transitions in the Hubbard [26,36,37] and transverse field Ising [18] chains. In two dimensions, s alone exhibits a kink.

We have shown that the HK model, in the vicinity of the Mott transition in one dimension, is less entangled than free fermions. Although neither ground state develops two-point entanglement in higher dimensions $d > 1$, a free Fermi surface is known to possess a large degree of entanglement between global bipartitions [23]. We expect that larger subsystems of the HK ground state will continue to exhibit less entanglement. This can be verified by constructing these states explicitly, building off of the present work, and numerically testing them for separability up to arbitrary precision [38].

Our local entropies should be understood in the context of the Hubbard model at finite temperature. Specifically in two dimensions, Walsh *et al.* have computed these entropies for the Hubbard model, using a combination of cluster dynamical mean-field theory and quantum Monte Carlo [25]. They found, at low temperatures, an interaction-driven Mott transition that is markedly distinct from the HK transition, being first-order instead of continuous. At their lowest temperatures, the Hubbard model's entropy density s vanishes in the insulator and jumps discontinuously to $\approx \frac{1}{5}\ln 2$ at the transition before smoothly decaying in the metal, whereas its single-site entropy s_1 increases monotonically from $\approx \frac{8}{5}\ln 2$ in the insulator to the metal, with a jump discontinuity of $\approx \frac{1}{10}\ln 2$ at the transition. Following our earlier discussion of the subadditivity bound $2s_1 \geq s_2 \geq 2s$, this is strong evidence for increasing spatial correlations in the Hubbard metal, as one expects. The only obstruction is the fine-tuned possibility that $I(j:\bar{j}) = (s_1 - s) - ((L^d - 1)s - s_{L^d-1})$ remains constant while $s_1 - s$ increases. Now the HK metal exhibits a classical entropy s that similarly decreases and a single-site entropy s_1 that is instead constant throughout, resulting in a qualitatively similar increase in the discrepancy $s_1 - s$. Quantitatively, in the vicinity of their respective Mott transitions, the Hubbard metal has $s_1 - s \approx \frac{3}{2}\ln 2$, larger than the HK metal's $s_1 - s \approx \ln 2$. We have extended this analysis to the next smallest subsystem, with $s_2 - 2s \sim 2\ln 2 + (\ln 16) c_d \delta u^{d/2}$ also increasing in the HK metal. The two models are primarily distinguished on the basis of coupling between high- and low-energy d.o.f. in their Hamiltonians: coupling with doubly occupied modes in the Hubbard model is known to result in dynamical spectral weight transfer, whereas the absence of any such coupling in the HK model results in its static double occupancy. We expect that this distinction can explain (at least qualitative) differences in local correlations between the two models.

ACKNOWLEDGMENTS

We are thankful to helpful comments from B. Langley and the NSF DMR-1461952 for partial funding of this project.

APPENDIX: MATRIX ELEMENTS OF THE TWO-SITE DENSITY MATRIX

We compute the matrix elements of the two-site density matrix

$$\rho^{\langle jj'\rangle} = \mathrm{diag}(p_{0,0}, \rho_{1,0}, \rho_{0,1}, \rho_{1,1}, p_{2,0}, p_{0,2}, \rho_{2,1}, \rho_{1,2}, p_{2,2}) \tag{A1}$$

[4]Recall that this bound is sufficiently general to apply also to this mixed state generated by nonlocal interactions. The mutual information $I(A:B)$—between two subsystems A and B in the state ρ^{AB}—is a relative entropy $S(\rho^{AB}\|\rho^A \otimes \rho^B) = I(A:B)$ from the state $\rho^A \otimes \rho^B$ with $\rho^{A,B} = \mathrm{tr}_{B,A}\rho^{AB}$, constructed to remove exactly those correlations between A and B. We use the quantum Pinsker inequality $S(\rho\|\sigma) \geq \frac{1}{2}(\|\rho - \sigma\|_1)^2$ and a Hölder inequality $||\rho^{AB}||_1 \geq \mathrm{tr}(\rho^{AB} O_A O_B)$ for operators O_I supported only on $I = A, B$ and normalized such that its largest singular value $||O_I||_\infty \leq 1$ is bounded by unity. Then

$$I(A:B)|_{\rho^{AB}} \geq \frac{1}{2}\left(\frac{\langle O_A O_B\rangle - \langle O_A\rangle\langle O_B\rangle}{\|O_A\|_\infty \|O_B\|_\infty}\right) \tag{47}$$

with expectation values taken in the state ρ^{AB}.

which is block diagonal in the particle number decomposition

$$\mathcal{H}_j \otimes \mathcal{H}_{j'} = \mathrm{Span}\{|0,0\rangle\} \tag{A2}$$

$$\oplus\, \mathrm{Span}\{|\uparrow,0\rangle, |0,\uparrow\rangle\} \oplus \mathrm{Span}\{|\downarrow,0\rangle, |0,\downarrow\rangle\} \tag{A3}$$

$$\oplus\, \mathrm{Span}\{|\uparrow,\downarrow\rangle, |\downarrow,\uparrow\rangle, |\uparrow\downarrow,0\rangle, |0,\uparrow\downarrow\rangle\} \tag{A4}$$

$$\oplus\, \mathrm{Span}\{|\uparrow,\uparrow\rangle\} \oplus \mathrm{Span}\{|\downarrow,\downarrow\rangle\} \tag{A5}$$

$$\oplus\, \mathrm{Span}\{|\uparrow\downarrow,\uparrow\rangle, |\uparrow,\uparrow\downarrow\rangle\}$$
$$\oplus\, \mathrm{Span}\{|\uparrow\downarrow,\downarrow\rangle, |\downarrow,\uparrow\downarrow\rangle\} \tag{A6}$$

$$\oplus\, \mathrm{Span}\{|\uparrow\downarrow,\uparrow\downarrow\rangle\}. \tag{A7}$$

In the one-dimensional subspaces, the diagonal elements are

$$p_{2,2} = \langle n_{j\uparrow} n_{j\downarrow} n_{j'\uparrow} n_{j'\downarrow}\rangle, \tag{A8}$$

$$p_{0,0} = \langle (1-n_{j\downarrow})(1-n_{j'\downarrow})(1-n_{j\uparrow})(1-n_{j'\uparrow})\rangle \tag{A9}$$

$$= 2\langle n_{j\uparrow} n_{j'\uparrow}\rangle - 4\langle n_{j\uparrow} n_{j\downarrow} n_{j'\uparrow}\rangle + p_{2,2}, \tag{A10}$$

$$p_{2,0} = \langle (1-n_{j\downarrow}) n_{j'\downarrow} n_{j\uparrow} n_{j'\uparrow}\rangle \tag{A11}$$

$$= \langle n_{j\uparrow} n_{j'\uparrow}\rangle - 2\langle n_{j\uparrow} n_{j\downarrow} n_{j'\uparrow}\rangle + p_{2,2}, \tag{A12}$$

$$p_{0,2} = p_{2,0}. \tag{A13}$$

In the two-dimensional subspaces,

$$\rho_{2,1} = \begin{pmatrix} p_{\uparrow\downarrow,\uparrow} & \zeta \\ \zeta^* & p_{\uparrow,\uparrow\downarrow} \end{pmatrix} \tag{A14}$$

$$\text{where } p_{\uparrow,\uparrow\downarrow} = p_{\uparrow\downarrow,\uparrow} = \langle n_{j\uparrow} n_{j\downarrow} n_{j'\uparrow}(1-n_{j'\downarrow})\rangle \tag{A15}$$

$$= \langle n_{j\uparrow} n_{j\downarrow} n_{j'\uparrow}\rangle - p_{2,2}, \tag{A16}$$

$$\zeta = \langle n_{j\uparrow} n_{j'\uparrow} c^\dagger_{j\downarrow} c_{j'\downarrow}\rangle, \tag{A17}$$

and

$$\rho_{1,0} = \begin{pmatrix} p_{\uparrow,0} & \zeta' \\ \zeta'^* & p_{0,\uparrow} \end{pmatrix} \tag{A18}$$

$$\text{where } p_{0,\uparrow} = p_{\uparrow,0} = \langle (1-n_{j\downarrow})(1-n_{j'\downarrow}) n_{j\uparrow}(1-n_{j'\uparrow})\rangle \tag{A19}$$

$$= -\langle n_{j\uparrow} n_{j'\uparrow}\rangle + 3\langle n_{j\uparrow} n_{j\downarrow} n_{j'\uparrow}\rangle - p_{2,2}, \tag{A20}$$

$$\zeta' = \langle (1-n_{j\downarrow})(1-n_{j'\downarrow}) c^\dagger_{j\uparrow} c_{j'\uparrow}\rangle \tag{A21}$$

$$= \langle c^\dagger_{j\uparrow} c_{j'\uparrow}\rangle - 2\langle n_{j\downarrow} c^\dagger_{j\uparrow} c_{j'\uparrow}\rangle + \zeta, \tag{A22}$$

in addition to $\rho_{1,2} = \rho_{2,1}$ and $\rho_{0,1} = \rho_{1,0}$.

In the only four-dimensional subspace,

$$\rho_{1,1} = \begin{pmatrix} p_{\uparrow,\downarrow} & x & w & w^* \\ x^* & p_{\downarrow,\uparrow} & -w & -w^* \\ w^* & -w^* & p_{\uparrow\downarrow,0} & x' \\ w & -w & x'^* & p_{0,\uparrow\downarrow} \end{pmatrix} \tag{A23}$$

where

$$p_{\downarrow,\uparrow} = p_{\uparrow,\downarrow} = \langle (1-n_{j\downarrow})(1-n_{j'\uparrow}) n_{j\uparrow} n_{j'\downarrow}\rangle \tag{A24}$$

$$= 1/4 - 2\langle n_{j\uparrow} n_{j\downarrow} n_{j'\uparrow}\rangle + p_{2,2}, \tag{A25}$$

$$p_{0,\uparrow\downarrow} = p_{\uparrow\downarrow,0} = \langle (1-n_{j'\uparrow})(1-n_{j'\downarrow}) n_{j\uparrow} n_{j\downarrow}\rangle \tag{A26}$$

$$= 1/4 - 2\langle n_{j\uparrow} n_{j\downarrow} n_{j'\uparrow}\rangle + p_{2,2}, \tag{A27}$$

$$x = \langle c^\dagger_{j'\downarrow} c^\dagger_{j\uparrow} c_{j\downarrow} c_{j'\uparrow}\rangle, \tag{A28}$$

$$x' = \langle c^\dagger_{j\downarrow} c^\dagger_{j\uparrow} c_{j'\uparrow} c_{j'\downarrow}\rangle, \tag{A29}$$

$$w = \langle (1-n_{j'\uparrow}) n_{j\uparrow} c^\dagger_{j'\downarrow} c_{j\downarrow}\rangle \tag{A30}$$

$$= \langle n_{j'\downarrow} c^\dagger_{j\uparrow} c_{j'\uparrow}\rangle^* - \zeta^*. \tag{A31}$$

We see that all matrix elements can be written in terms of $p_{2,2}$, ζ, x, x', $\langle c^\dagger_{j\uparrow} c_{j'\uparrow}\rangle$, $\langle n_{j\downarrow} c^\dagger_{j\uparrow} c_{j'\uparrow}\rangle$, $\langle n_{j\uparrow} n_{j'\uparrow}\rangle$, $\langle n_{j\uparrow} n_{j'\downarrow}\rangle$, and $\langle n_{j\uparrow} n_{j\downarrow} n_{j'\uparrow}\rangle$. The simplest of these are

$$\langle n_{j\uparrow} n_{j'\downarrow}\rangle = \frac{1}{L^{2d}} \sum_{kp} p_\pi \sum_\pi \langle n_{k\uparrow}\rangle_\pi \langle n_{p\downarrow}\rangle_\pi \tag{A32}$$

$$= p_{\uparrow\downarrow} \tag{A33}$$

$$= 1/4 \tag{A34}$$

$$= \langle n_{j\uparrow}\rangle \langle n_{j'\downarrow}\rangle \tag{A35}$$

and $z = \langle c^\dagger_{j\uparrow} c_{j'\uparrow}\rangle$, already computed in the text.

Some algebra leads to

$$\langle n_{j\uparrow} n_{j'\uparrow}\rangle = \frac{1}{L^{2d}} \sum_{k,k'} (1 - e^{-i(k-k')(j-j')}) \mathbb{E}_2(k,k'), \tag{A36}$$

$$\langle c^\dagger_{j'\downarrow} c^\dagger_{j\uparrow} c_{j\downarrow} c_{j'\uparrow}\rangle = x = -\frac{1}{L^{2d}} \sum_{k,p} e^{-i(k-p)(j-j')} \mathbb{E}_2(k,p), \tag{A37}$$

$$\langle c^\dagger_{j\downarrow} c^\dagger_{j\uparrow} c_{j'\uparrow} c_{j'\downarrow}\rangle = x' = \frac{1}{L^{2d}} \sum_{k,p} e^{-i(k+p)(j-j')} \mathbb{E}_2(k,p), \tag{A38}$$

$$\langle n_{j'\downarrow} c^\dagger_{j\uparrow} c_{j'\uparrow}\rangle = \langle n_{j\downarrow} c^\dagger_{j\uparrow} c_{j'\uparrow}\rangle = \frac{1}{L^{2d}} \sum_{kp} e^{-ik(j-j')} \mathbb{E}_2(k,p), \tag{A39}$$

$$\langle n_{j\uparrow} n_{j\downarrow} n_{j'\uparrow}\rangle = \frac{1}{L^{3d}} \sum_{k,k',p} (1 - e^{-i(k-k')(j-j')}) \mathbb{E}_3(k,k',p), \tag{A40}$$

$$\langle n_{j\uparrow} n_{j'\uparrow} c^\dagger_{j\downarrow} c_{j'\downarrow}\rangle = \zeta = \frac{1}{L^{3d}} \sum_{k,k',p} e^{-ip(j-j')} (1 - e^{-i(k-k')(j-j')}) \times \mathbb{E}_3(k,k',p), \tag{A41}$$

$$p_{2,2} = \frac{1}{L^{4d}} \sum_{k,k',p,p'} (1 - e^{-i(k-k')\cdot(j-j')}) \times (1 - e^{-i(p-p')\cdot(j-j')}) \mathbb{E}_4(k,k',p,p'), \tag{A42}$$

where

$$\mathbb{E}_2(k,k') = p_\pi \sum_\pi \langle n_{k\sigma}\rangle_\pi \langle n_{k'\sigma'}\rangle_\pi, \tag{A43}$$

$$\mathbb{E}_3(k,k',p) = p_\pi \sum_\pi \langle n_{k\uparrow}\rangle_\pi \langle n_{k'\uparrow}\rangle_\pi \langle n_{p\downarrow}\rangle_\pi, \tag{A44}$$

$$\mathbb{E}_4(k,k',p,p') = p_\pi \sum_\pi \langle n_{k\uparrow}\rangle_\pi \langle n_{k'\uparrow}\rangle_\pi \langle n_{p\downarrow}\rangle_\pi \langle n_{p'\downarrow}\rangle_\pi \tag{A45}$$

factorize, for distinct momenta in the thermodynamic limit, as

$$\mathbb{E}_2(k \in \Omega_a, k' \in \Omega_b) = \frac{a}{2}\frac{b}{2}, \tag{A46}$$

$$\mathbb{E}_3(k \in \Omega_a, k' \in \Omega_b, p \in \Omega_c) = \frac{a}{2}\frac{b}{2}\frac{c}{2}, \tag{A47}$$

$$\mathbb{E}_4(k \in \Omega_a, k' \in \Omega_b, p \in \Omega_c, p' \in \Omega_d) = \frac{a}{2}\frac{b}{2}\frac{c}{2}\frac{d}{2}. \tag{A48}$$

Since the phase space of distinct momenta dominates the Fourier sums in the thermodynamic limit, one can read from the above expressions that all matrix elements of the two-site reduced state $\rho^{\langle jj'\rangle}$ factorize as described in the text, so $\rho^{\langle jj'\rangle} = \rho^{jj'\uparrow} \otimes \rho^{jj'\downarrow}$ also factorizes. Then the single-site reduced state also factorizes as $\rho^j = \rho^{j\uparrow} \otimes \rho^{j\downarrow}$.

[1] A. B. Harris and R. V. Lange, Phys. Rev. **157**, 295 (1967).
[2] M. B. J. Meinders, H. Eskes, and G. A. Sawatzky, Phys. Rev. B **48**, 3916 (1993).
[3] P. Phillips, Rev. Mod. Phys. **82**, 1719 (2010).
[4] H. Eskes and A. M. Oleś, M. B. J. Meinders, and W. Stephan, Phys. Rev. B **50**, 17980 (1994).
[5] C. T. Chen, F. Sette, Y. Ma, M. S. Hybertsen, E. B. Stechel, W. M. C. Foulkes, M. Schulter, S.-W. Cheong, A. S. Cooper, L. W. Rupp, B. Batlogg, Y. L. Soo, Z. H. Ming, A. Krol, and Y. H. Kao, Phys. Rev. Lett. **66**, 104 (1991).
[6] D. C. Peets, D. G. Hawthorn, K. M. Shen, Y.-J. Kim, D. S. Ellis, H. Zhang, S. Komiya, Y. Ando, G. A. Sawatzky, R. Liang, D. A. Bonn, and W. N. Hardy, Phys. Rev. Lett. **103**, 087402 (2009).
[7] S. Uchida, T. Ido, H. Takagi, T. Arima, Y. Tokura, and S. Tajima, Phys. Rev. B **43**, 7942 (1991).
[8] S. L. Cooper, G. A. Thomas, J. Orenstein, D. H. Rapkine, A. J. Millis, S.-W. Cheong, A. S. Cooper, and Z. Fisk, Phys. Rev. B **41**, 11605 (1990).
[9] A. F. Santander-Syro, R. P. S. M. Lobo, N. Bontemps, Z. Konstantinovic, Z. Z. Li, and H. Raffy, Europhys. Lett. **62**, 568 (2003).
[10] H. J. A. Molegraaf, C. Presura, D. van der Marel, P. H. Kes, and M. Li, Science **295**, 2239 (2002).
[11] M. Rübhausen, A. Gozar, M. V. Klein, P. Guptasarma, and D. G. Hinks, Phys. Rev. B **63**, 224514 (2001).
[12] Y. Hatsugai and M. Kohmoto, J. Phys. Soc. Jpn. **61**, 2056 (1992).
[13] G. Baskaran, Mod. Phys. Lett. B **05**, 643 (1991).
[14] R. Horodecki, P. Horodecki, M. Horodecki, and K. Horodecki, Rev. Mod. Phys. **81**, 865 (2009).
[15] H. Casini and M. Huerta, Phys. Lett. B **600**, 142 (2004).
[16] P. Zanardi and X. Wang, J. Phys. A **35**, 7947 (2002).
[17] P. Zanardi, Phys. Rev. A **65**, 042101 (2002).
[18] T. J. Osborne and M. A. Nielsen, Phys. Rev. A **66**, 032110 (2002).
[19] B. Swingle, Phys. Rev. Lett. **105**, 050502 (2010).
[20] H. Casini and M. Huerta, J. Phys. A **42**, 504007 (2009).
[21] I. Peschel and V. Eisler, J. Phys. A **42**, 504003 (2009).
[22] I. Peschel and V. Eisler, J. Phys. A **42**, 504003 (2009).
[23] D. Gioev and I. Klich, Phys. Rev. Lett. **96**, 100503 (2006).
[24] T. Faulkner, A. Lewkowycz, and J. Maldacena, J. High Energy Phys. 11 (2013) 74.

[25] C. Walsh, P. Sémon, D. Poulin, G. Sordi, and A.-M. S. Tremblay, Phys. Rev. B **99**, 075122 (2019).
[26] D. Larsson and H. Johannesson, Phys. Rev. A **73**, 042320 (2006).
[27] M. A. Continentino, Phys. Rev. B **45**, 11312 (1992).
[28] M. A. Continentino and M. D. Coutinho-Filho, Solid State Commun. **90**, 619 (1994).
[29] I. Dzyaloshinskii, Phys. Rev. B **68**, 085113 (2003).
[30] A. Rosch, Eur. Phys. J. B **59**, 495 (2007).
[31] K. B. Dave, P. W. Phillips, and C. L. Kane, Phys. Rev. Lett. **110**, 090403 (2013).
[32] K. Modi, A. Brodutch, H. Cable, T. Paterek, and V. Vedral, Rev. Mod. Phys. **84**, 1655 (2012).
[33] F. S. Nogueira and E. V. Anda, Int. J. Mod. Phys. B **10**, 3705 (1996).
[34] S. Sachdev and J. Ye, Phys. Rev. Lett. **70**, 3339 (1993).
[35] A. Kitaev, http://online.kitp.ucsb.edu/online/entangled15/kitaev/ (2015).
[36] S.-J. Gu, Y.-Q. Li, and H.-Q. Lin, Phys. Rev. Lett. **93**, 086402 (2004).
[37] D. Larsson and H. Johannesson, Phys. Rev. Lett. **95**, 196406 (2005).
[38] F. Brandão, M. Christandl, and J. Yard, in *Proceedings of the Forty-Third Annual ACM Symposium on Theory of Computing, San Jose, California, USA* (ACM, New York, 2011), p. 343, http://doi.acm.org/10.1145/1993636.1993683.